UNCOVERING BIOLOGICAL MOTIFS AND SYNTAX VIA SUFFICIENT AND NECESSARY EXPLANATIONS

Anonymous authors
Paper under double-blind review

ABSTRACT

Deep neural networks (DNNs) have achieved remarkable success in predicting transcription factor (TF) binding from high-throughput genome profiling data. Since TF binding is primarily driven by sequence motifs, understanding how DNNs make accurate predictions could help identify these motifs and their logical syntax. However, the black-box nature of DNNs complicates interpretation. Most post-hoc methods evaluate the importance of each base pair in isolation, often resulting in noise since they overlook the fact that motifs are contiguous regions. Additionally, these methods fail to capture the complex interactions between different motifs. To address these challenges, we propose Motif Explainer Models (MEMs), a novel explanation method that uses sufficiency and necessity to identify important motifs and their syntax. MEMs excel at identifying multiple disjoint motifs across DNA sequences, overcoming limitations of existing methods. Moreover, by accurately pinpointing sufficient and necessary motifs, MEMs can reveal the logical syntax that governs genomic regulation.

1 INTRODUCTION

The regulatory function of DNA sequences is determined by short DNA segments called "motifs", where certain proteins called "transcription factors" (TFs) bind to regulate gene activity (Klug, 1995; Alberts et al., 2002; Siggers & Gordân, 2014; Lambert et al., 2018). TF binding depends on the arrangement and logical combination of these motifs. High-throughput experiments provide a genome-wide view of regulatory activity in various cell types (Consortium et al., 2012). Techniques like DNase-seq and ATAC-seq identify regions of open chromatin where TFs can bind, while more targeted methods like ChIP-seq offer insights into specific protein–DNA interactions.

Given the complexity and volume of data from these experiments, accurately predicting genome activity from DNA sequences requires models that can handle large datasets and capture the intricate interactions and arrangement of motifs. Deep neural networks (DNNs), with their proven success in various biological sequence prediction tasks, are well-suited for this challenge. They have achieved state-of-the-art performance in predicting TF binding from DNA sequences (Alipanahi et al., 2015; Avsec et al., 2021; Eraslan et al., 2019). Genomic DNNs take DNA sequences as inputs and learn to predict a label from a regulatory profiling experiment, such as whether a TF binds to a given sequence. The goal is to use these accurate models to identify the motifs and syntax governing genomic regulation (Novakovsky et al., 2023).

Despite their success, the black-box nature of these models makes it difficult to understand how and why they make specific predictions (Zednik, 2021; Tomsett et al., 2018). In regulatory genomics, this has led to the development of post-hoc methods to explain genomic DNNs at the local (sample) level. Given a model f and an input N-length DNA sequence $\mathbf{x} = (x_1, x_2, \ldots, x_N) \in \mathbb{R}^N$, these methods aim to identify important motifs for the prediction $f(\mathbf{x})$ by assigning an importance score to each base pair x_i, and then segmenting out high-importance regions as putative motifs. However, many of these methods fall short because they evaluate the importance of individual base pairs in *isolation*, and do not leverage the fact that motifs are short, contiguous regions. Furthermore, these methods also fail to capture the complex interactions between motifs.

To address these challenges, Linder et al. (2022) introduced *scramblers*, a model-based explanation method optimized for the discrete nature of biological sequences. Scramblers outperform traditional post-hoc methods by identifying important motifs using learned stochastic masks. However, when the input is a complex DNA sequence with multiple motifs, scramblers struggle to identify multiple

short contiguous regions as they do not leverage the key properties of motifs we know of. Due to this shortcoming, like other methods, scramblers cannot adequately uncover the logical syntax governing regulatory behavior.

In this work, we propose a novel model-based explanation method called *Motif Explainer Models* (MEMs), which leverages notions of sufficiency and necessity to produce meaningful explanations. For complex DNA sequences composed of disjoint and contiguous motifs, we show that MEMs accurately identify motifs and outperform the current state-of-the-art method of scramblers. Furthermore, by employing sufficient and necessary explanations together, we demonstrate that MEMs can reveal the logical syntax between motifs that governs genomic regulation.

1.1 Summary of Our Contributions

We address the challenges of interpreting genomic DNNs by proposing a novel model-based explanation method that can identify important motifs and deduce their logical syntax. Specifically, our methodology identifies both sufficient or necessary motifs, providing more accurate and interpretable explanations for genomic DNNs on complex DNA sequences. Our contributions include:

1. Motif Explainer Models (MEMs): We introduce *Motif Explainer Models* (MEMs), a model-based explanation method capable of generating sufficient or necessary explanations for genomic DNNs. MEMs can handle disjoint and contiguous motifs gracefully, capturing the intricate arrangements and interactions that other methods miss.
2. Uncovering Logical Syntax via Sufficiency and Necessity: By combining sufficient and necessary explanations, we show that MEMs can reveal the logical syntax governing how motifs interact to regulate downstream gene expression.
3. Experimental Validation: Through a series of experiments, we demonstrate that MEMs outperform scramblers, the current state-of-the-art method in identifying important motifs. Additionally, we show how MEMs can deduce common biological syntactical rules, such as cooperation, repression, and redundancy.

1.2 Related Works

A comprehensive overview of related works is presented in Appendix A.1.

2 Background

Notation. Random vectors and their observed values are denoted with uppercase (e.g., $\mathbf{X}$) and lowercase (e.g., $\mathbf{x}$) letters. For a subset of features $S \subseteq [N]$ (where $[N] \coloneqq \{1, \ldots, N\}$), we denote its complement as $\bar{S} = [N] \setminus S$. Additionally, subscripts index features, e.g. the vector $\mathbf{x}_S$ is the restriction of $\mathbf{x}$ to the components indexed by S. The input domain of N-length DNA sequences and output domain of binary labels are denoted as $\mathcal{X} = \{\texttt{A}, \texttt{C}, \texttt{G}, \texttt{T}\}^N$ and $\mathcal{Y} = \{0, 1\}$, respectively. A distribution over features and labels $\mathcal{X} \times \mathcal{Y}$ is denoted as $\mathcal{D}$ and the marginal distribution over features is represented as $\mathcal{D}_{\mathcal{X}}$. Lastly, denote $\rho : \mathbb{R} \times \mathbb{R} \mapsto \mathbb{R}$ to be any symmetric function that measures the similarity between elements $a, b \in \mathbb{R}$ with the property $\rho(a, b) = 0 \iff a = b$. A common choice is $\rho(a, b) = (a - b)^2$, which we use in our experiments.

Setting. We consider a binary classification setting with a distribution $\mathcal{D}$ over $\mathcal{X} \times \mathcal{Y}$, a domain of N-length DNA sequences and binary labels. Since the inputs are N-length DNA sequences, when we refer to an input DNA sequence $\mathbf{x}$, note it is implicitly being expressed as a one-hot encoded pattern, $\mathbf{x} \in \{0, 1\}^{N \times 4}$ (a N-length sequence of alphabet size 4, representing the 4 base pairs $\{\texttt{A}, \texttt{C}, \texttt{G}, \texttt{T}\}$). We assume access to a predictor $f : \mathcal{X} \mapsto \mathcal{Y}$, pretrained on DNA sequence–label pairs, $(\mathbf{X}, Y) \sim \mathcal{D}$. Our goal of interpretation is: for a fixed DNA sequence $\mathbf{x}$, identify which short subsequences, i.e. motifs, in $\mathbf{x}$ are most important for the prediction $f(\mathbf{x})$. To do so, our method—as with many other post-hoc methods (Covert et al., 2021; Fong & Vedaldi, 2017; Fong et al., 2019)—relies on evaluating how a predictor's behavior changes when base-pairs in $\mathbf{x}$ are retained or omitted. Since f can only accept N-length sequences as an input we employ the standard technique for querying f on subsets of features by evaluating the *average restricted prediction*

$$f_S(\mathbf{x}) = \mathop{\mathbb{E}}_{\mathbf{X}_{\bar{S}} \sim \mathcal{V}_{\bar{S}}} [f(\mathbf{x}_S, \mathbf{X}_{\bar{S}})] \tag{1}$$

where $\mathbf{x}_S$ is fixed and $\mathbf{X}_{\bar{S}}$ is a random vector sampled from $\mathcal{V}_{\bar{S}}$ an arbitrary reference distribution over the features indexed by $\bar{S}$ (Covert et al., 2021; Teneggi et al., 2023; Bharti et al., 2025).

2.1 SUFFICIENCY AND NECESSITY

Our methodology takes as input a pretrained predictor $f : \mathcal{X} \mapsto \mathcal{Y}$ and a fixed DNA sequence $\mathbf{x}$, and outputs a subset $S \subseteq [d]$ that is considered "important" for the prediction $f(\mathbf{x})$. We define the importance of S using slightly modified notions of sufficiency and necessity originally proposed by Bharti et al. (2025). We present our modified definitions, below for clarity:

Definition 1 (Sufficiency & Necessity (Bharti et al., 2025)). *Let ϵ and $\Delta > 0$. Denote $\rho : \mathbb{R} \times \mathbb{R} \mapsto \mathbb{R}$ to be a similarity measure. For a predictor f and sample $\mathbf{x}$, denote $\hat{Y}(\mathbf{x}) = \mathbb{1}[f(\mathbf{x}) \geq 0.5]$ to be the predicted class of $\mathbf{x}$.*

A subset $S \subseteq [d]$ is ϵ-sufficient with respect to distribution $\mathcal{V}$ for f at $\mathbf{x}$ if

$$\rho(\hat{Y}(\mathbf{x}), f_S(\mathbf{x})) \leq \epsilon \tag{2}$$

A subset $S \subseteq [d]$ is Δ-necessary with respect to a distribution $\mathcal{V}$ for f at $\mathbf{x}$ if

$$\rho(\hat{Y}(\mathbf{x}), f_{\bar{S}}(\mathbf{x})) \geq \Delta. \tag{3}$$

In other words, for a reference distribution $\mathcal{V}$, a subset of features S is ϵ-sufficient if, with $\mathbf{x}_S$ fixed, the average restricted prediction $f_S(\mathbf{x})$ is ϵ close to the predicted class $\hat{Y}(\mathbf{x})$. Conversely, a subset of features S is Δ-necessary if, when the features in S are marginalized out, the resulting average restricted prediction $f_{\bar{S}}(\mathbf{x})$ is Δ away from $\hat{Y}(\mathbf{x})$. Later in this work, we will illustrate why sufficient *and* necessary explanations are essential for deducing motif syntax and how our method accurately identifies sufficient and necessary motifs. Furthermore, we show that while scramblers generate these explanations with some success, our proposed method achieves far greater accuracy, enabling more reliable deduction of the underlying motifs and their logical syntax.

2.2 SCRAMBLERS

Given a pre-trained predictor f and fixed DNA-sequence $\mathbf{x}$, a scrambler (Linder et al., 2022) is a learned model $g : \mathcal{X} \mapsto \mathbb{R}^N_{>0}$ that predicts a set of real-valued importance scores in $(0, \infty]^N$. These scores produce a probability distribution $P_g(\mathbf{x})$ that we can sample from. Specifically, $P_g(\mathbf{x})$ is a set of N categorical softmax-nodes, also known as a position-specific scoring matrix (PSSM) that interpolates between $\mathbf{x} \in \{0, 1\}^{N \times 4}$ and a non-informative background distribution $\tilde{B} \in [0, 1]^{N \times 4}$. One can learn a scrambler g by solving the following optimization problem

$$\underset{g \subseteq \mathcal{H}}{\arg\min} \quad \mathop{\mathbb{E}}_{\mathbf{X} \sim \mathcal{D}_{\mathcal{X}}} \left[L(f, \mathbf{X}, P_g) + \lambda \cdot \left(t_{\text{bits}} - \frac{1}{N} \text{KL} \left[\tilde{B} || P_g(\mathbf{X}) \right] \right)^2 \right] \tag{4}$$

where $L(f, \mathbf{X}, P_g)$ denotes a loss function, $\left(t_{\text{bits}} - \frac{1}{N} \text{KL} \left[\tilde{B} || P_g(\mathbf{X}) \right] \right)^2$ a conservation penalty, and $\lambda > 0$ a hyperparameter which controls the magnitude of the penalty. Depending on the type of scrambler to be learned, the loss function $L(f, \mathbf{X}, P_g)$ and functional form of probability distribution $P_g(\mathbf{X})$ will vary. There are two types of scramblers, an inclusion scrambler and occlusion scrambler which aim to identify sufficient and necessary motifs respectively.

Inclusion Scrambler. An *inclusion* scrambler is trained with

$$L(f, \mathbf{X}, P_g) = \mathop{\mathbb{E}}_{\tilde{\mathbf{X}} \sim P_g(\mathbf{X})} \left[\text{KL} \left[f(\tilde{\mathbf{X}}) || f(\mathbf{X}) \right] \right] \quad \text{and} \quad P_g(\mathbf{x}) = \sigma(\log(\tilde{B}) + \mathbf{x} \times \dot{g}(\mathbf{x})). \tag{5}$$

where σ denotes the softmax $\sigma(L)_{ij} = \frac{\exp(L_{ij})}{\sum_{k=1}^{M} \exp(L_{ik})}$ and $\dot{g}(\mathbf{x}) \in (0, \infty]^{N \times M}$ represent the scores $g(\mathbf{x})$ broadcasted across the base (ACGT) dimension. With these choices of $L(f, \mathbf{X}, P_g)$, conservation penalty, small value of t_{bits}, and $P_g(\mathbf{x})$, an inclusion scrambler is trained to output scores in $(0, \infty]^N$ which produce a distribution $P_g(\mathbf{x})$ whose cross entropy relative to $\tilde{B}$ is small, but whose samples $\tilde{\mathbf{X}} \sim P_g(\mathbf{x})$ minimize the predictive reconstructive error, $\mathop{\mathbb{E}}_{\tilde{\mathbf{X}} \sim P_g(\mathbf{X})} \left[\text{KL} \left[f(\tilde{\mathbf{X}}) || f(\mathbf{X}) \right] \right]$, thus identifying sufficient features.

Occlusion Scrambler. An *occlusion* scrambler is trained with

$$L(f, \mathbf{X}, P_g) = - \mathop{\mathbb{E}}_{\tilde{\mathbf{X}} \sim P_g(\mathbf{X})} \left[\text{KL} \left[f(\tilde{\mathbf{X}}) || f(\mathbf{X}) \right] \right] \quad \text{and} \quad P_g(\mathbf{x}) = \sigma(\log(\tilde{B}) + \mathbf{x} / \dot{g}(\mathbf{x})). \tag{6}$$

With these choices of $L(f, \mathbf{X}, P_g)$, conservation penalty, appropriately chosen value for t_{bits}, and $P_g(\mathbf{x})$ an occlusion scrambler is trained to output scores in $(0, \infty]^N$ which produce a distribution $P_g(\mathbf{x})$ whose cross entropy relative to $\tilde{B}$ is approximately t_{bits}, and whose samples $\tilde{\mathbf{X}} \sim P_g(\mathbf{x})$ maximize the predictive reconstructive error. Since the samples from $P_g(\mathbf{x})$ maximize the reconstructive error, this formulation identifies necessary features.

2.3 Shortcomings of Scramblers

While scramblers outperform common post-hoc methods in providing explanations, they still face some key limitations that affect their overall effectiveness.

Lack of Key Prior Knowledge. DNA motifs are generally recognized as small, contiguous, and disjoint subsequences within a larger sequence (Klug, 1995; Alberts et al., 2002; Siggers & Gordân, 2014; Lambert et al., 2018; Stormo, 2013; Maston et al., 2006). Thus, incorporating this key information as an inductive bias into explanation methods could greatly improve the quality of the identified motifs. However, scramblers do not explicitly consider this prior knowledge; instead, they learn a distribution $P_g(\mathbf{X})$ over sequences, which optimizes jointly for the prediction reconstruction error and for entropy. While this formulation is valid to produce necessary or sufficient explanations, it fails to capture prior knowledge of motif biology, particularly that motifs occur as one or more small, contiguous, and disjoint subsequences.

Limitations of the Conservation Penalty. While inclusion and occlusion scramblers aim to maximize and minimize the entropy of $P_g(\mathbf{x})$ via the conservation penalty, their effectiveness heavily depends on the choice of the t_{bits} parameter. This parameter controls the entropy and serves as the target value for the expected entropy of $P_g(\mathbf{X})$. For example, a larger t_{bits} allows more entropy for $P_g(\mathbf{x})$ with respect to the background $\tilde{B}$. For an inclusion scrambler, $t_{\text{bits}} \approx 0$ is appropriate. However, for an occlusion scrambler, choosing t_{bits} can be challenging. This is because we often do not know how many motifs exist or how distinct they are from the background signal, making it difficult to determine an appropriate target entropy for $P_g(\mathbf{x})$ relative to $\tilde{B}$. Additionally, considering our prior knowledge of motif biology, there is no theoretically justifiable reason that enforcing entropy will lead to the identification of small, contiguous motifs, which we will demonstrate in our experimental section.

3 Motif Explainer Models

To address the limitations of scramblers and provide more accurate explanations that highlight contiguous and disjoint motifs, we propose *Motif Explainer Models* (MEMs). This model-based based explanation approach is designed to incorporate the key properties of motifs, better capturing the structure and arrangement of motifs within sequences, and offering a more precise and biologically meaningful interpretation. A MEM is a model $m : \mathcal{X} \mapsto [0, 1]^N$ that outputs importance scores in $[0, 1]^N$. For a sequence $\mathbf{x} = (x_1, \ldots, x_n)$, a MEM outputs scores $m(\mathbf{x}) = (m_1, \ldots, m_N)$ that produce a probability distribution $P_m(\mathbf{x})$ over the random variable $\tilde{\mathbf{X}} = (\tilde{X}_1, \ldots, \tilde{X}_N)$ where

$$\Pr[\tilde{X}_i = x_i] = m_i \quad \text{and} \quad \Pr[\tilde{X}_i = b_i] = 1 - m_i \tag{7}$$

i.e., $\tilde{X}_i \sim \text{Bernoulli}(m_i)$ with outcomes $\{x_i, b_i\}$. Here b_i are entries of a vector $\mathbf{b} \in \mathcal{X}$, a background vector used to fill the entries of $\tilde{\mathbf{X}}$. A MEM is learned by solving the following general optimization problem

$$\underset{m \subseteq \mathcal{H}}{\arg\min} \quad \mathop{\mathbb{E}}_{\mathbf{X} \sim \mathcal{D}_{\mathcal{X}}} \left[L(f, \mathbf{X}, P_g) + R(m(\mathbf{X})) \right] \tag{8}$$

Here, $L(f, \mathbf{X}, P_m)$ is a loss function that measures the reconstruction error between original predictions $f(\mathbf{X})$ and predictions on the samples from $P_m(\mathbf{X})$. The term $R(m(\mathbf{X}))$ is a regularizer that controls the complexity of the MEM outputs. There are two types of MEMs that can be learned: a sufficient MEM (s-MEM) and a necessary MEM (n-MEM), depending on the choice of loss function $L(f, \mathbf{X}, P_M)$. The regularizer R remains the same for both types of MEMs.

Loss Function. The choice of loss function determines whether one wants to learn a s-MEM or n-MEM. To learn an s-MEM the loss function is:

$$L(f, \mathbf{X}, P_m) = \rho\left(f(\mathbf{x}), \mathbb{E}[f(\tilde{\mathbf{X}})]\right). \tag{9}$$

where, $\rho : \mathbb{R} \times \mathbb{R} \mapsto \mathbb{R}$ is a measure of similarity on $\mathbb{R}$ and the expectation is over P_m and $\mathbf{b}$ (if $\mathbf{b}$ is not fixed and instead sampled from some distribution). With this choice of L, an s-MEM minimizes the reconstruction error between the original prediction $f(\mathbf{X})$ and the average prediction over $P_m(\mathbf{X})$. Thus, an s-MEM is specifically designed to identify sufficient sets.

Conversely, a n-MEM is trained using the following loss function:

$$L(f, \mathbf{X}, P_m) = -\rho(f(\mathbf{x}), \mathbb{E}[f(\tilde{\mathbf{X}})]). \tag{10}$$

where the expectation is over $P_{(\mathbf{1}-m(\mathbf{x}))}$[1] and $\mathbf{b}$. Minimizing this loss is equivalent to maximizing $\rho(f(\mathbf{x}), \mathbb{E}[f(\tilde{\mathbf{X}})])$, the reconstruction error between a original predictions $f(\mathbf{X})$ and the average prediction over $P_{(\mathbf{1}-m(\mathbf{x}))}$. Therefore, an n-MEM is specifically designed to identify necessary sets.

Regularizers. Since motifs are known to be small, contiguous subsequences, we incorporate this key prior knowledge into our MEMs. Unlike scramblers, we regularize our models with an inductive bias that *directly* encourages the identification of disjoint, contiguous regions consisting of a limited number of base pairs. To construct the regularizer R, we draw inspiration from sentiment analysis in natural language processing. In NLP, disjoint clusters of words typically interact to convey sentiment; similarly, base pairs in DNA sequences interact to form motifs. Indeed, it has been shown that the syntactical structure of genome regulation has many similarities to natural language (Hwang et al., 2024). Following the approach of Brinner & Zarrieß (2023), we assume a linear coordinate system on DNA sequences $\mathbf{x}$ and define a distance $d(i, j)$ between base pairs i and j. With this assumed structure, instead of having our MEM directly outputting scores $m(\mathbf{x}) = (m_1, \dots m_N)$, we have it output two vectors $\mathbf{w} \in \mathbb{R}^N$ and $\sigma \in \mathbb{R}^N_{>0}$, and calculate the final scores as follows:

$$m_j = \text{sigmoid}\left(\sum_i w_{i,j}\right) \quad \text{where} \quad w_{i,j} = w_i \cdot \exp\left(-\frac{d(i,j)^2}{\sigma_i}\right)$$

Thus, the optimization is done with respect to $\mathbf{w}$ and σ. As noted by (Brinner & Zarrieß, 2023), this parametrization of $m(\mathbf{X})$ will encourage neighboring base-pairs to be assigned similar scores if the corresponding σ values are large. With this parametrization, the final regularizer R defined as

$$R(m(\mathbf{X})) = \lambda_1 \cdot ||m(\mathbf{X})||_1 - \lambda_2 \cdot \frac{1}{N}\sum_i \log(\sigma_i), \tag{11}$$

where $|| \cdot ||_1$ is the ℓ_1 norm and large σ values are promoted with the additional term $\lambda_2 \cdot \frac{1}{N}\sum_i \log(\sigma_i)$. The first term encourages the importance scores to be sparse, meaning only a small number of base pairs are assigned high scores. The second term encourages neighboring importance scores to be similar while also promoting sharp boundaries when optimal. This is crucial because it allows for the discovery of disjoint contiguous regions, enabling a more accurate representation of the motifs and their distinct properties.

4 Experimental Results

In the following experiments, we demonstrate that MEMs accurately identify motifs and help infer logical syntax. We compare MEMs to scramblers, the standard model-based explanation method: s-MEMs to inclusion scramblers, which generate sufficient explanations, and n-MEMs to occlusion scramblers, which generate necessary explanations. Since prior work has shown that scramblers outperform traditional post-hoc methods, we focus our comparison on MEMs and scramblers.

4.1 Synthetic Data

We conduct experiments on synthetic DNA sequences $\mathbf{x} \in \{0, 1\}^{500\times 4}$ containing two motifs, A and B, which correspond to the SPI1 and CTCF DNA-binding motifs of 10 and 12 base pairs, respectively (Friedman, 2007; Pchelintsev et al., 2016). We model three common logical syntax rules—cooperation, repression, and redundancy—to determine the labels $Y \in \{0, 1\}$. For all three logical rules, our label predictor f is a residual network with dilated convolutions. To ensure a fair comparison between MEMs and scramblers, we normalize scrambler attribution scores to $[0, 1]$ by computing their information content (Shannon, 1948) and applying min-max normalization. The

[1] $\mathbf{1}$ is the vector of all 1's in $\mathbb{R}^N$

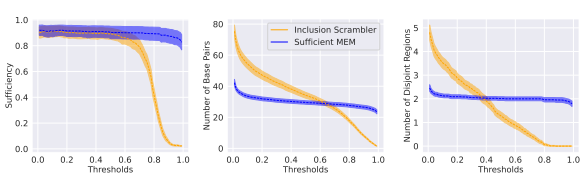

(a) s-MEMs vs. inclusion scramblers

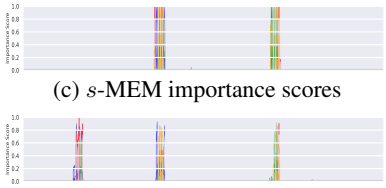

(c) s-MEM importance scores

(d) Inclusion scrambler importance scores

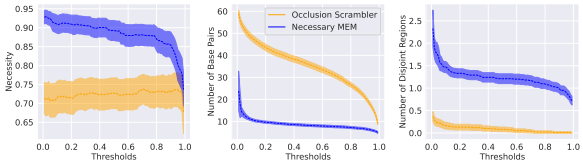

(b) n-MEMs vs. occlusion scramblers

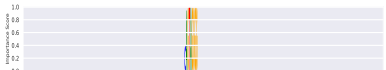

(e) n-MEM importance scores

(f) Occlusion scrambler importance scores

Figure 1: Results on positively labeled sequences ($Y = 1$) under a cooperative syntax

resulting importance scores are thresholded for $t \in (0, 1)$ to define solution sets S_t. Each S_t is represented as a binary vector $s_t \in \{0, 1\}^{500}$, where $(s_t)_j = 1$ if $j \in S_t$ and 0 otherwise.

To compare MEMs and scramblers, we quantify and report key metrics for the explanations S_t on a hold-out set of sequences. We measure the sufficiency and necessity of S_t using $1 - |\hat{Y}(\mathbf{x}) - f_{S_t}(\mathbf{x})|$ and $|\hat{Y}(\mathbf{x}) - f_{\bar{S}_t}(\mathbf{x})|$, respectively, where $\hat{Y}(\mathbf{x})$ is the predicted class of model f. Higher values indicate greater sufficiency and necessity of S_t. Additionally, we quantify the number of base pairs in S_t as $|S_t| = ||s_t||_0$ and count the number of disjoint regions by identifying clusters of consecutive '1's in s_t. Since, we a prior do not know which threshold generates the explanation S_t, we compute our metrics for all $t \in (0, 1)$. As a result, the effectiveness of MEMs and scramblers is evaluated based on their ability to generate high-quality explanations across all possible thresholds. We will show that, unlike MEMs, scrambler performance is highly sensitive to t, and in any experiment, there is no single t for which scramblers outperform MEMs. Further experimental details are provided in Appendix A.3.

4.2 Learning Logical Syntax

We consider the three following types of logical syntax between motifs. These three arguably constitute the vast majority of syntactical constraints between motifs in regulatory biology. We present the results for the cooperative and redundant syntax and defer repression to Appendix A.2.

Cooperative

$$Y = \begin{cases} 1 & \text{if } A \wedge B \\ 0 & \text{otherwise} \end{cases}$$

Redundant

$$Y = \begin{cases} 1 & \text{if } A \vee B \\ 0 & \text{otherwise} \end{cases}$$

Repressive

$$Y = \begin{cases} 1 & \text{if } A \wedge \neg B \\ 0 & \text{otherwise} \end{cases}$$

4.2.1 Cooperative Syntax

We begin with a data-generating process that follows a cooperative syntax, where a $Y = 1$ label is assigned only when both motifs A and B are present; otherwise, the label is negative. Consequently, for a predictor trained on this rule, the set $\{A, B\}$ is sufficient for positive predictions, as both motifs are required to produce a positive label. Conversely, among positive predictions, either $\{A\}$ or $\{B\}$ is necessary, since removing either results in a changed prediction.

In Fig. 1a, we compare the effectiveness of s-MEMs and inclusion scramblers in explaining the predictor and recovering the correct set of sufficient motifs. For the sequences with true label $Y = 1$, the results show that for thresholds $t \in (0, 0.6)$, both methods successfully identify sufficient features. However, as t increases, the inclusion scrambler struggles to recover the sufficient set. Notably, the s-MEM is more accurate and outperforms the inclusion scrambler because it identifies two motifs as being sufficient for the predictor. Across all $t \in (0, 1)$, the s-MEM identifies approximately 20–30 important base pairs across 2–3 disjoint regions, while the inclusion scrambler detects between 0 and 80 base pairs, with 0-5 regions depending on the threshold t.

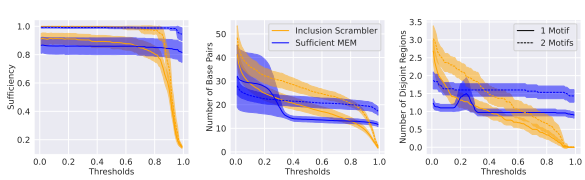

(a) s-MEMs vs. inclusion scramblers

(c) S-MEM importance scores

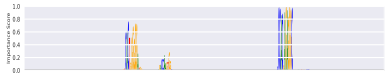

(d) Inclusion scrambler importance scores

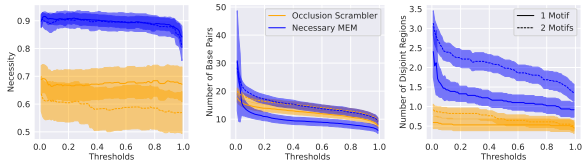

(b) n-MEMs vs. occlusion scramblers

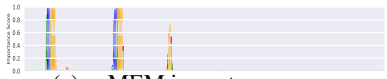

(e) n-MEM importance scores

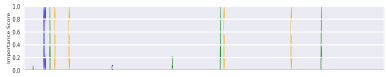

(f) Occlusion scrambler importance scores

Figure 2: Results on positively labeled sequences ($Y = 1$) under a redundant syntax

In Fig. 1b, we compare the effectiveness of n-MEMs and occlusion scramblers in recovering the correct necessary motifs. The results indicate that, for all thresholds both methods identify necessary regions, with the n-MEM detecting more necessary regions. More importantly though, the n-MEM identifies regions which the scrambler misses. The n-MEM is identifying 0-20 important base-pairs dispersed over 1–1.5 regions, while the scrambler is detecting anywhere from 0-60 base-pairs dispersed randomly, as indicated by its identifying 0-0.5 regions on average. Examples are provided in Figs. 1e and 1f.

Importantly, combining the interpretations from our s-MEM and n-MEM enables us to accurately and robustly deduce that the logical syntax underpinning the system is *cooperation*. That is, 2 motifs are sufficient and 1 is necessary for a positive prediction. Thus, MEMs allow the identification of logical rules between motifs.

4.2.2 Redundant Syntax

We next consider a redundant syntax setting. This rule assigns a positive label if either A, B, or both are present, and a negative label otherwise. As a result, for a predictor that effectively learns this rule, either the sets $\{A\}$ and $\{B\}$ are sufficient since the true data-generating process assigns a positive label when either motif is present. On the other hand, depending on whether a sequence contains either A or B or both, the set of necessary motifs may vary. For sequences that contain both, the set $\{A, B\}$ is necessary since only when both are removed will the predictor generate predictions that yield a classification $= 0$. For a sequence that contains only A (or B), the set $\{A\}$ (or $\{B\}$) is necessary as the removal of this single motif will render the label $Y = 0$.

In Fig. 2b, we compare s-MEMs and inclusion scramblers in a redundant setting. The results show that for thresholds $t \in (0, 0.9)$, both methods identify sufficient regions; however, as t increases, the inclusion scrambler struggles to recover sufficient regions. Notably, for sequences labeled $Y = 1$ due to a single motif (either A or B), both methods identify sets that are slightly less sufficient compared to those for positively labeled sequences containing both motifs. More importantly though, for the $Y = 1$ sequences with a single motif, the s-MEM is able to detect 1 disjoint region for nearly all t while the inclusion scrambler identifies more regions for smaller t and less regions for large t. Likewise, for sequences with a ground truth of two motifs, the s-MEM detects 20-30 base-pairs that are dispersed in 1.5 to 2 regions. Note, theoretically, one motif is sufficient to predict the positive label but the s-MEM identifies a bit more. We attribute this to the s-MEM's learning that there are two motifs present in this sequence and it attributing some importance to the second motif.

In Fig. 2e, we highlight how n-MEMs are able to identify necessary motifs with much greater success than occlusion scramblers. The results show that across all thresholds, both methods identify necessary regions, with n-MEMs identifying regions that are much more necessary. Additionally, n-MEMs are able to accurately detect the correct the number of motifs among the two modes of the ground truth (i.e., whether there is 1 or 2 motifs). As expected, for sequences with two motifs, our

n-MEM identifies 10–30 base-pairs over 2–2.5 regions for many t, while for sequences with only one motif, the n-MEM identifies 5-10 base-pairs that make up 1–1.5 regions to be necessary. On the other hand, the occlusion scrambler fails to distinguish these details. Instead, it outputs the same (incorrect) explanations for both modes of the ground truth, identifying 20–30 base pairs over 0.5–1 regions to be necessary.

Thus, by combining interpretations from an s-MEM and an n-MEM, we can accurately identify that 1 motif is sufficient and 1–2 motifs are necessary (depending on the sequence) for a positive prediction. Therefore, we can conclude this setting indeed follows a redundant syntax.

5 Experimental Data

We use the CTCF (HepG2) dataset from the ENCODE project to analyze CTCF binding sites in the HepG2 cell line and their role in protein-DNA interactions (Consortium et al., 2012). This dataset contains 500 base pair DNA sequences with associated IDR peaks from a ChIP-seq experiment.

Our model f is a residual network with dilated convolutions, achieving 76% accuracy on a hold-out test set. The results in Table 1 compare the explanations of MEMs and scramblers. We compute the cosine similarity between IDR peak profiles and explanations generated by MEMs and scramblers. A high cosine similarity indicates that MEM and scrambler explanations assign relative importance to base pairs in a manner that closely matches the IDR peak profile.

Following our synthetic experiments, we also evaluate sufficiency and the number of base pairs identified. Both s-MEMs and inclusion scramblers identify sufficient regions with similar alignment to the IDR peak profile. The key difference is that s-MEMs identify much smaller regions, indicating they can more accurately pinpoint sufficient motifs compared to inclusion scramblers.

We omit a comparison between n-MEMs and occlusion scramblers because these methods frequently produce attributions that fail to align with actual motif base pairs. We attribute this to the noisy nature of the experimental data and the fragility of the model f. These properties can result in a few random base pairs being "necessary," since even small perturbations can cause significant changes in model predictions.

	Cosine Similarity	Sufficiency	Number of Base Pairs
s-MEM	0.294 ± 0.041	0.979 ± 0.005	36.314 ± 3.802
Inclusion Scrambler	0.327 ± 0.036	0.974 ± 0.005	59.952 ± 6.996

Table 1: Comparison of s-MEM and Inclusion Scrambler

6 Conclusion & Future Directions

In this work, we introduced Motif Explainer Models (MEMs), a novel explanation method for genomic DNNs that identifies both sufficient and necessary motifs in complex DNA sequences. In contrast to current methods like scramblers, MEMs leverage prior domain knowledge as an inductive bias to cleanly identify individual motifs as disjoint and contiguous subsequences. Furthermore, by discovering sufficient and necessary motifs separately, MEMs address the limitations of existing post-hoc methods that often fail to capture the intricate logical relationships between motifs. Our approach not only improves the interpretability of genomic DNNs, but also uncovers the logical syntax governing gene regulation, distinguishing between as cooperative, repressive, and redundant interactions.

Through extensive experiments, we demonstrated that MEMs outperform current methods in detecting important motifs and deciphering their underlying syntax. By providing more accurate and comprehensive explanations, MEMs offer new insights into the functional roles of motifs in gene regulation, paving the way for better understanding of transcription-factor binding and genomic activity. In summary, MEMs represent a significant step forward in interpreting complex genomic models, offering a robust framework for elucidating the logic behind motif interactions. Future work may explore extending this framework to more diverse regulatory contexts, ultimately enhancing our ability to interpret the functional landscape of the genome.

REFERENCES

Bruce Alberts, Alexander Johnson, Julian Lewis, Martin Raff, Keith Roberts, and Peter Walter. Dna-binding motifs in gene regulatory proteins. In *Molecular Biology of the Cell. 4th edition*. Garland Science, 2002.

Babak Alipanahi, Andrew Delong, Matthew T Weirauch, and Brendan J Frey. Predicting the sequence specificities of dna-and rna-binding proteins by deep learning. *Nature biotechnology*, 33 (8):831–838, 2015.

Žiga Avsec, Melanie Weilert, Avanti Shrikumar, Sabrina Krueger, Amr Alexandari, Khyati Dalal, Robin Fropf, Charles McAnany, Julien Gagneur, Anshul Kundaje, et al. Base-resolution models of transcription-factor binding reveal soft motif syntax. *Nature genetics*, 53(3):354–366, 2021.

Beepul Bharti, Paul Yi, and Jeremias Sulam. Sufficient and necessary explanations (and what lies in between). In *The Second Conference on Parsimony and Learning (Proceedings Track)*. PMLR, 2025.

Marc Brinner and Sina Zarrieß. Model interpretability and rationale extraction by input mask optimization. In *Findings of the Association for Computational Linguistics: ACL 2023*, pp. 13722–13744, 2023.

Jianbo Chen, Le Song, Martin J Wainwright, and Michael I Jordan. L-shapley and c-shapley: Efficient model interpretation for structured data. *arXiv preprint arXiv:1808.02610*, 2018.

ENCODE Project Consortium et al. An integrated encyclopedia of dna elements in the human genome. *Nature*, 489(7414):57, 2012.

Ian Covert, Scott Lundberg, and Su-In Lee. Explaining by removing: A unified framework for model explanation. *Journal of Machine Learning Research*, 22(209):1–90, 2021.

Gökcen Eraslan, Žiga Avsec, Julien Gagneur, and Fabian J Theis. Deep learning: new computational modelling techniques for genomics. *Nature Reviews Genetics*, 20(7):389–403, 2019.

Ruth Fong, Mandela Patrick, and Andrea Vedaldi. Understanding deep networks via extremal perturbations and smooth masks. In *Proceedings of the IEEE/CVF international conference on computer vision*, pp. 2950–2958, 2019.

Ruth C Fong and Andrea Vedaldi. Interpretable explanations of black boxes by meaningful perturbation. In *Proceedings of the IEEE international conference on computer vision*, pp. 3429–3437, 2017.

Alan D. Friedman. Transcriptional control of granulocyte and monocyte development. *The Journal of Experimental Medicine*, 204(8):1937–1943, 2007.

Amirata Ghorbani, Abubakar Abid, and James Zou. Interpretation of neural networks is fragile. In *Proceedings of the AAAI conference on artificial intelligence*, volume 33, pp. 3681–3688, 2019.

Yunha Hwang, Andre L. Cornman, Elizabeth H. Kellogg, Sergey Ovchinnikov, and Peter R. Girguis. Genomic language model predicts protein co-regulation and function. *Nature Communications*, 15(1):2880, 2024. URL `https://doi.org/10.1038/s41467-024-46947-9`.

Peng-Tao Jiang, Chang-Bin Zhang, Qibin Hou, Ming-Ming Cheng, and Yunchao Wei. Layercam: Exploring hierarchical class activation maps for localization. *IEEE Transactions on Image Processing*, 30:5875–5888, 2021.

David R Kelley, Jasper Snoek, and John L Rinn. Basset: learning the regulatory code of the accessible genome with deep convolutional neural networks. *Genome research*, 26(7):990–999, 2016.

Aaron Klug. Gene regulatory proteins and their interaction with dna. *Annals of the New York Academy of Sciences*, 758:143–160, 1995.

Samuel A Lambert, Arttu Jolma, Laura F Campitelli, Pratyush K Das, Yimeng Yin, Mihai Albu, Xiaoting Chen, Jussi Taipale, Timothy R Hughes, and Matthew T Weirauch. The human transcription factors. *Cell*, 172(4):650–665, 2018.

Johannes Linder, Alyssa La Fleur, Zibo Chen, Ajasja Ljubetič, David Baker, Sreeram Kannan, and Georg Seelig. Interpreting neural networks for biological sequences by learning stochastic masks. *Nature machine intelligence*, 4(1):41–54, 2022.

Scott M Lundberg and Su-In Lee. A unified approach to interpreting model predictions. *Advances in Neural Information Processing Systems*, 30, 2017.

Glenn A Maston, Stephanie K Evans, and Michael R Green. Transcriptional regulatory elements in the human genome. *Annual Review of Genomics and Human Genetics*, 7:29–59, 2006.

Gherman Novakovsky, Nick Dexter, Maxwell W Libbrecht, Wyeth W Wasserman, and Sara Mostafavi. Obtaining genetics insights from deep learning via explainable artificial intelligence. *Nature Reviews Genetics*, 24(2):125–137, 2023.

N. A. Pchelintsev et al. Ctcf: a key regulator of the 3d genome. *Current Opinion in Genetics Development*, 37:21–27, 2016.

Marco Tulio Ribeiro, Sameer Singh, and Carlos Guestrin. "why should i trust you?" explaining the predictions of any classifier. In *Proceedings of the 22nd ACM SIGKDD international conference on knowledge discovery and data mining*, pp. 1135–1144, 2016.

Ramprasaath R Selvaraju, Michael Cogswell, Abhishek Das, Ramakrishna Vedantam, Devi Parikh, and Dhruv Batra. Grad-cam: Visual explanations from deep networks via gradient-based localization. In *Proceedings of the IEEE international conference on computer vision*, pp. 618–626, 2017.

Claude E. Shannon. A mathematical theory of communication. *The Bell System Technical Journal*, 27:379–423, 623–656, 1948.

Avanti Shrikumar, Peyton Greenside, and Anshul Kundaje. Learning important features through propagating activation differences. In *International conference on machine learning*, pp. 3145–3153. PMLR, 2017.

Avanti Shrikumar, Katherine Tian, Žiga Avsec, Anna Shcherbina, Abhimanyu Banerjee, Mahfuza Sharmin, Surag Nair, and Anshul Kundaje. Technical note on transcription factor motif discovery from importance scores (tf-modisco) version 0.5. 6.5. *arXiv preprint arXiv:1811.00416*, 2018.

Trevor Siggers and Raluca Gordân. Protein–dna binding: complexities and multi-protein codes. *Nucleic acids research*, 42(4):2099–2111, 2014.

Karen Simonyan, Andrea Vedaldi, and Andrew Zisserman. Deep inside convolutional networks: Visualising image classification models and saliency maps. *arXiv preprint arXiv:1312.6034*, 2014.

Gary D. Stormo. Modeling the specificity of protein-dna interactions. *Quantitative Biology*, 1: 115–130, 2013.

Erik Strumbelj and Igor Kononenko. An efficient explanation of individual classifications using game theory. *The Journal of Machine Learning Research*, 11:1–18, 2010.

Mukund Sundararajan, Ankur Taly, and Qiqi Yan. Axiomatic attribution for deep networks. In *International conference on machine learning*, pp. 3319–3328. PMLR, 2017.

Jacopo Teneggi, Alexandre Luster, and Jeremias Sulam. Fast hierarchical games for image explanations. *IEEE Transactions on Pattern Analysis and Machine Intelligence*, 45(4):4494–4503, 2022.

Jacopo Teneggi, Beepul Bharti, Yaniv Romano, and Jeremias Sulam. Shap-xrt: The shapley value meets conditional independence testing. *Transactions on Machine Learning Research*, 2023.

Richard Tomsett, Dave Braines, Dan Harborne, Alun Preece, and Supriyo Chakraborty. Interpretable to whom? a role-based model for analyzing interpretable machine learning systems. *arXiv preprint arXiv:1806.07552*, 2018.

Alex Tseng, Avanti Shrikumar, and Anshul Kundaje. Fourier-transform-based attribution priors improve the interpretability and stability of deep learning models for genomics. *Advances in Neural Information Processing Systems*, 33:1913–1923, 2020.

Alex M Tseng, Gökcen Eraslan, Nathaniel Lee Diamant, Tommaso Biancalani, and Gabriele Scalia. A mechanistically interpretable neural-network architecture for discovery of regulatory genomics. In *ICLR 2024 Workshop on Machine Learning for Genomics Explorations*, 2024.

Jason Yosinski, Jeff Clune, Anh Nguyen, Thomas Fuchs, and Hod Lipson. Understanding neural networks through deep visualization. In *Deep Learning Workshop, International Conference on Machine Learning (ICML)*, 2015.

Carlos Zednik. Solving the black box problem: a normative framework for explainable artificial intelligence. *Philosophy & Technology*, 34(2):265–288, 2021.

Matthew D Zeiler and Rob Fergus. Visualizing and understanding convolutional networks. In *European conference on computer vision*, pp. 818–833. Springer, 2014.

Bolei Zhou, Aditya Khosla, Agata Lapedriza, Aude Oliva, and Antonio Torralba. Learning deep features for discriminative localization. In *Proceedings of the IEEE conference on computer vision and pattern recognition*, pp. 2921–2929, 2016.

Jian Zhou and Olga G Troyanskaya. Predicting effects of noncoding variants with deep learning–based sequence model. *Nature methods*, 12(10):931–934, 2015.

A Appendix

A.1 Related Works

Several methods have been proposed for discovering motifs from genomic DNNs.

Visualizing Convolutional Filters. Most DNNs used for sequence prediction tasks are convolutional neural networks. (Alipanahi et al., 2015; Zhou & Troyanskaya, 2015; Kelley et al., 2016; Avsec et al., 2021). Thus, to identify important motifs, many works simply visualize CNN filters (Alipanahi et al., 2015; Kelley et al., 2016) as early convolutional layers often capture basic patterns, while deeper layers capture more complex features (Zeiler & Fergus, 2014; Yosinski et al., 2015; Simonyan et al., 2014). However, this approach has shown limited success, as it assumes each filter learns one motif, and that each motif is learned by only one filter. Recent research shows that motifs are distributed across multiple filters and layers (Tseng et al., 2024).

Measuring Influence via Post-hoc Explanation Methods. Popular post-hoc explanation methods like CAM (Zhou et al., 2016), LIME (Ribeiro et al., 2016), gradient-based approaches (Selvaraju et al., 2017; Shrikumar et al., 2017; Jiang et al., 2021), Shapley value-based methods (Chen et al., 2018; Teneggi et al., 2022), and perturbation-based methods (Fong & Vedaldi, 2017; Fong et al., 2019) have been adapted to identify motifs. These methods assign importance scores to each base pair (Sundararajan et al., 2017; Shrikumar et al., 2017), but they perform poorly for two reasons. First, by assigning scores to base pairs individually, they miss key motifs because base pairs and subsequences of subsequences of base pairs inherently interact in complex ways to regulate function. Second, these methods are computationally expensive. For instance, integrated gradients and DeepLIFT integrate over the entire DNN, while Shapley-based methods require exponential computations (Strumbelj & Kononenko, 2010; Lundberg & Lee, 2017). These shortcomings render the importance scores noisy and fragile. As a result, they fail to reveal the model's true decision-making process (Ghorbani et al., 2019; Tseng et al., 2020), making it difficult to rely on downstream tools like MoDISco to cluster them into motifs (Shrikumar et al., 2018).

Scramblers. To overcome these limitations of traditional post-hoc methods, Linder et al. (2022) proposed scramblers, a model-based explanation method that learns stochastic masks to highlight the base pairs crucial for predictions. Scramblers predict position-specific scoring matrices (PSSMs), where unimportant base pairs are "scrambled" by increasing their entropy. Scramblers have a distinct advantage over many traditional post-hoc explanation methods due to their model-based approach: a scrambler only needs to be trained once for any model predictive f, after which importance scores for any query DNA sequence can be obtained in a single evaluation. While scramblers outperform other post-hoc methods, they still struggle with sequences composed of multiple disjoint and contiguous motifs. This is due to a regularization penalty that focuses on controlling entropy, rather than incorporating the core characteristics of motifs (small, contiguous, and disjoint). As a result, scramblers are limited in complex settings and fail to uncover the logical syntax of motif interactions for genomic regulation.

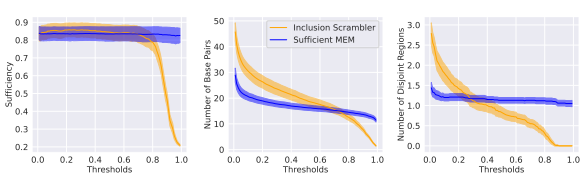

(a) s-MEMs vs. inclusion scramblers

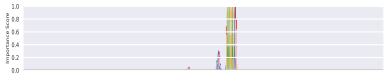

(c) s-MEM importance scores

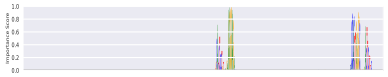

(d) Inclusion scrambler importance scores

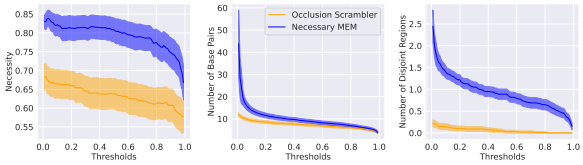

(b) n-MEMs vs. occlusion scramblers

(e) n-MEM importance scores

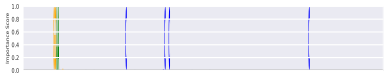

(f) Occlusion scrambler importance scores

Figure 3: Results on positively labeled sequences ($Y = 1$) under a repressive syntax

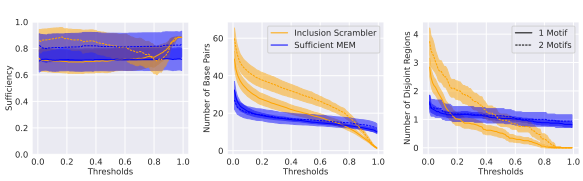

(a) s-MEMs vs. inclusion scramblers

(c) s-MEM importance scores

(d) Inclusion scrambler importance scores

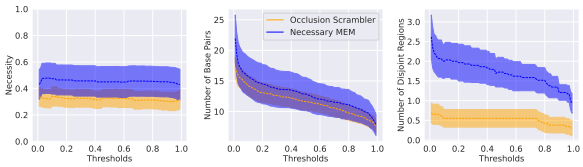

(b) n-MEMs vs. occlusion scramblers

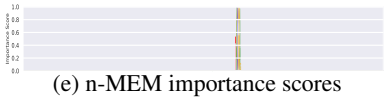

(e) n-MEM importance scores

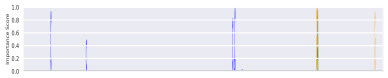

(f) Occlusion scrambler importance scores

Figure 4: Results on negatively labeled sequences ($Y = 0$) under a repressive syntax

A.2 Additional Experiments

A.2.1 Repressive Syntax

Lastly, we consider a data-generating process based on a repressive syntax. This rule assigns a positive label if M_1 is present and M_2 is absent, and a negative label in all other cases. The logic in this rule is more involved as M_2 represses M_1 from generating a positive label. In this setting, for sequences with $Y = 1$, the smallest sufficient and necessary set is $\{M_1\}$ since its sole presence results in a positive classification and removal in a negative classification. On the other hand, for negatively labeled sequences $Y = 0$, the logic is more involved. When the negative label is due to both M_1 and M_2 being present, the sufficient and necessary set is M_2 because its presence yields the correct negative prediction and its removal results in a positive label. For the subset of negatively labeled sequences that contains M_2 only, the set $\{M_2\}$ is both sufficient and necessary.

In Figs. 3a and 3b, we compare the ability of MEMs and scramblers to identify the sufficient and necessary motifs on sequences with $Y = 1$. In, Fig. 3a we see for thresholds $t \in (0, 0.8)$, both methods identify sufficient regions but as t continues to increase, the inclusion scrambler fails to recover sufficient regions. Furthermore, the s-MEM outperforms the scrambler for $t \in (0, 0.8)$ in correctly identifying a single motif. The s-MEM identifies 15–30 important base pairs dispersed over 1–1.5 regions, while the scrambler inaccurately identifies 15–50 important base pairs dispersed over anywhere from 0.5–3 regions. In Fig. 3b, both n-MEMs and occlusion scramblers identify necessary base-pairs with the n-MEM identifying those that are more necessary. Interestingly, the occlusion scramblers identify a smaller number of important base-pairs. However, for $t \in [0.1, 0.9]$

the n-MEM detects 0.5–1.5 regions while the occlusion detects nearly no regions on average. This suggests that the occlusion scrambler is erroneously identifying random base-pairs as necessary and not the actual important motifs. One can see an example of this in Fig. 3f

In Fig. 4b, we highlight how n-MEMs are able to indeed identify necessary motifs for the subpopulation of sequences that have label $Y = 0$ due to the presence of both A and B. The results show that both methods identify necessary regions, with n-MEMs identifying regions that are more necessary. Additionally, both methods identify roughly the same number of important base-pairs, which ranges form 5-25. However, the n-MEM is able to discern that there are 1-2 important regions (i.e. the B motif) while the occlusion scrambler cannot, as evidenced by its identifying 0–1 important regions. An example of this is illustrated in Fig. 4f

In conclusion, by using an s-MEM and n-MEM, we are able to accurately discern that, for positive predictions, one motif (A) is both sufficient and necessary. Additionally, for negative predictions, there exists a sub population of sequences that for which one motif, B, is sufficient. Furthermore, among this sub-population there exists sequences for which 1 motif, B, is necessary where removing it generates a positive prediction, (implying A was repressed by B). Thus, we can ultimately deduce that this setting indeed follows a repression syntax.

A.3 Additional Experimental Details

Implementation of MEMs. To learn MEMs we solve the following optimization problem

$$\underset{m \subseteq \mathcal{H}}{\arg\min} \quad \mathop{\mathbb{E}}_{\mathbf{X} \sim \mathcal{D}_{\mathcal{X}}} [L(f, \mathbf{X}, P_g) + \lambda \cdot R(m(\mathbf{X}))] \tag{12}$$

To learn s-MEMS we let

$$L(f, \mathbf{X}, P_m) = (\hat{Y}(\mathbf{X}) - \mathbb{E}_{P_m}[f(\tilde{\mathbf{X}})])^2 \tag{13}$$

and to learn n-MEMS we let

$$L(f, \mathbf{X}, P_m) = -(\hat{Y}(\mathbf{X}) - \mathbb{E}_{P_{\mathbf{1}-m}}[f(\tilde{\mathbf{X}})])^2. \tag{14}$$

We solve this problem via empirical risk minimization. Given N samples $\{\mathbf{X}_i\}_{i=1}^N \overset{\text{i.i.d.}}{\sim} \mathcal{D}_X$, we learn a model m to minimize

$$\frac{1}{N} \sum_{i=1}^{N} [L(f, \mathbf{X}_i, P_m) + \lambda \cdot R(m(\mathbf{X}_i))] \tag{15}$$

where

$$\mathbb{E}[f(\tilde{\mathbf{X}}_\mathbf{i})] = \frac{1}{K} \sum_{j=1}^{K} f((\tilde{\mathbf{X}}_i)_j). \tag{16}$$

In theory, the entries of $(\tilde{\mathbf{X}}_i)_j$ are Bernoulli(m_i) with outcomes $\{x_i, b_i\}$. where b_i are entries of a vector $\mathbf{b} \in \mathcal{X}$, a background vector used to fill the entries of $\tilde{\mathbf{X}}$. In practice, to allow for differentiaion during optimization, we generate approximately discrete samples using the Gumbel-Softmax distribution. During optimization we set $K = 10$.

Recall the form of regularizer

$$R(m(\mathbf{X})) = \lambda_1 \cdot ||m(\mathbf{X})||_1 - \lambda_2 \cdot \frac{1}{N} \sum_i \log(\sigma_i). \tag{17}$$

To learn MEMs use a residual network with dilated convolutions. To learn s-MEMs, we set $\lambda_1 = 2$ and $\lambda_2 = 0.5$. To learn n-MEMs, we set $\lambda_1 = 5$ and $\lambda_2 = 0.01$. We used a batch size of 32 and trained for each MEM for 25 epochs using an Adam optimizer with default β-parameters of $\beta_1 = 0.9$, $\beta_2 = 0.99$ and a fixed learning rate of 0.001.

Implementation of Scramblers. To learn inclusion and occlusion scramblers we simply follow the protocol in Linder et al. (2022) and use a residual network with dilated convolutions. To learn inclusion scramblers, we set $\lambda = 2$ and $t_{\text{bits}} = 1 \times 10^{-4}$. To learn occlusion scramblers, we set $\lambda = 5$ and $t_{\text{bits}} = 1 \times 10^{-4}$. We use a batch size of 32 and train for 25 epochs using an Adam optimizer with default β-parameters of $\beta_1 = 0.9$, $\beta_2 = 0.99$ and a fixed learning rate of 0.001.

A.4 ADDITIONAL FIGURES

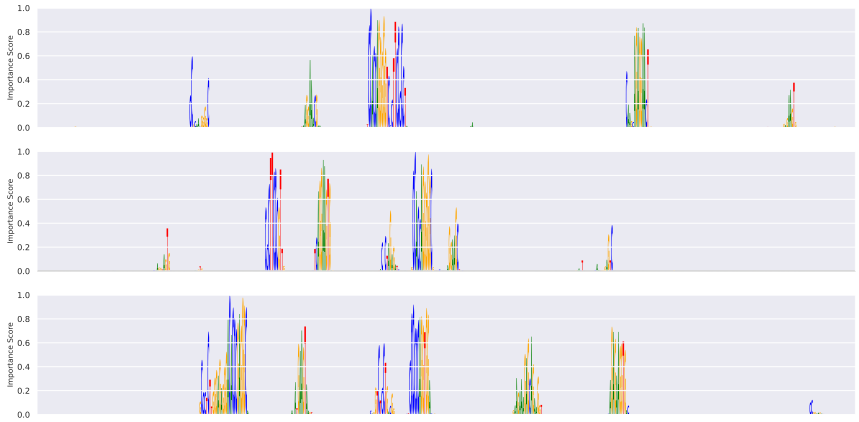

Figure 5: Inclusion scrambler importance scores for a cooperative syntax

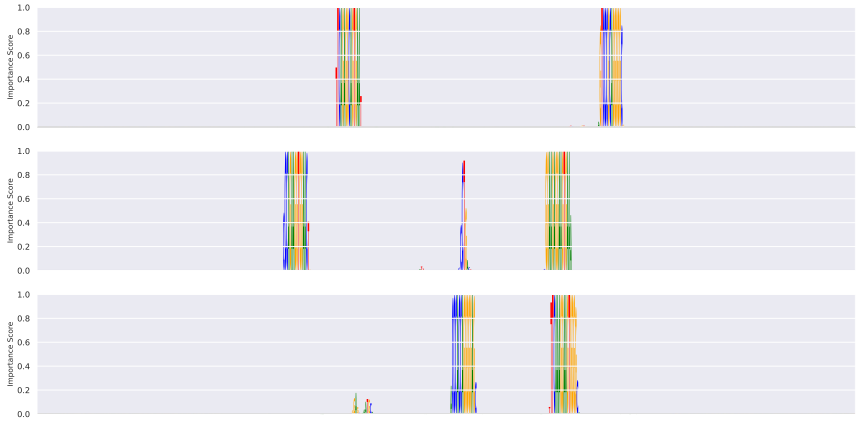

Figure 6: s-MEM importance scores for a cooperative syntax

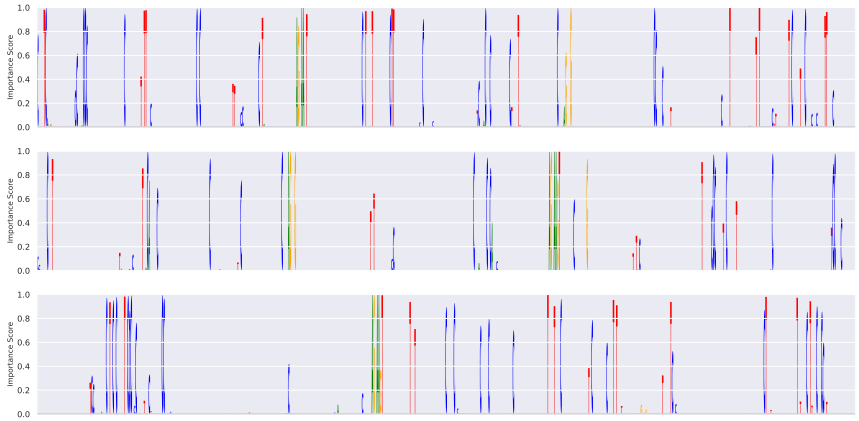

Figure 7: Occlusion scrambler importance scores for a cooperative syntax

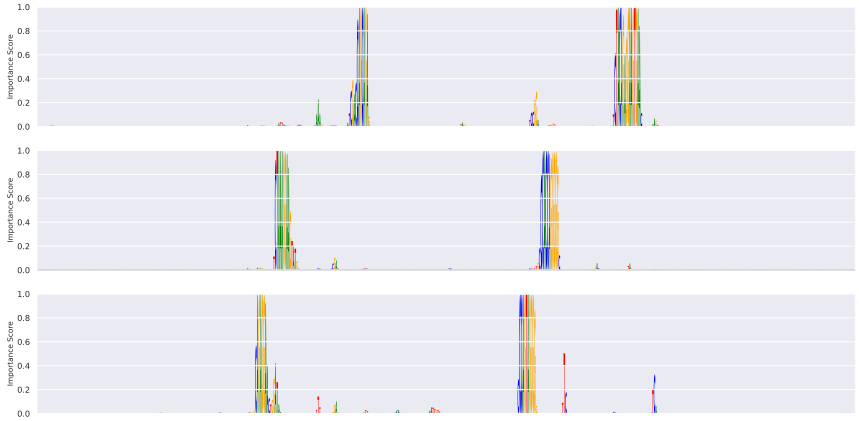

Figure 8: n-MEM importance scores for a cooperative syntax

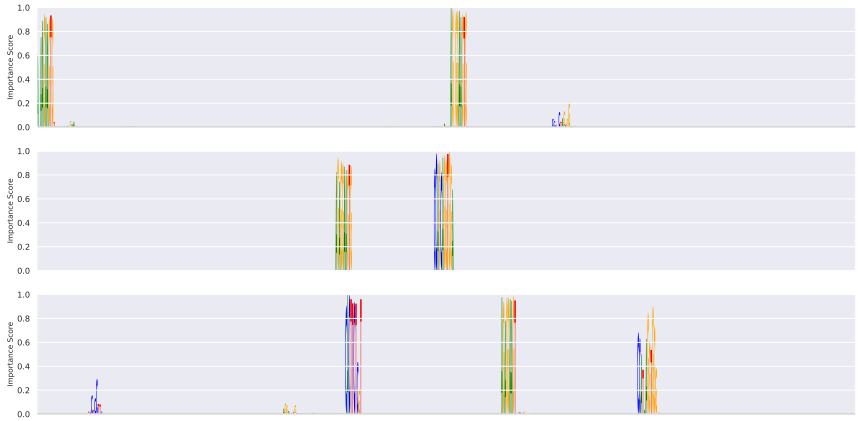

Figure 9: Inclusion scrambler importance scores for a redundant syntax

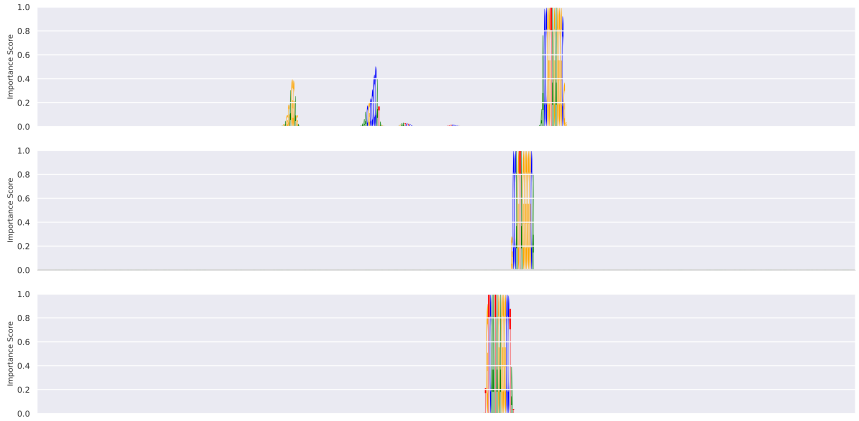

Figure 10: s-MEM importance scores for a redundant syntax

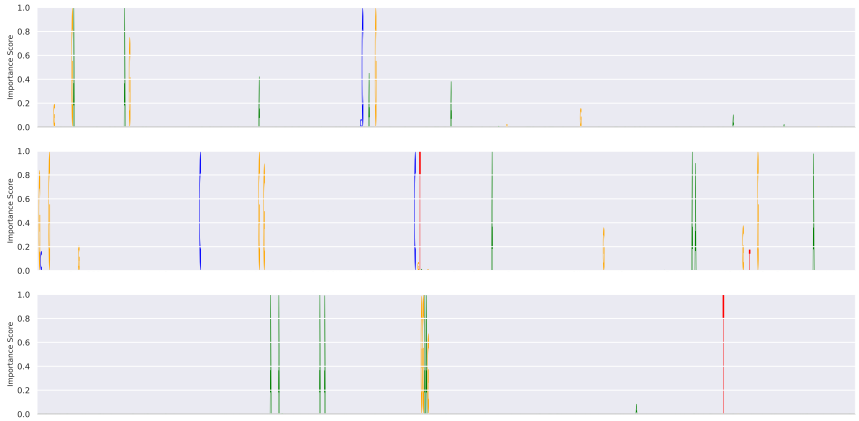

Figure 11: Occlusion scrambler importance scores for a redundant syntax

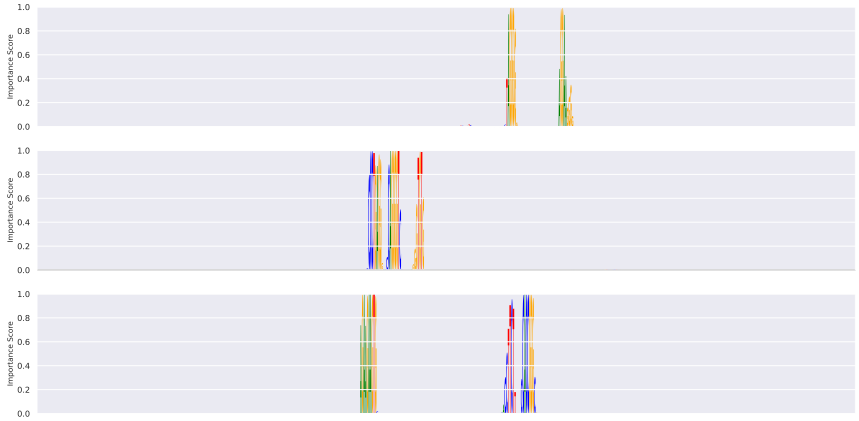

Figure 12: n-MEM importance scores for a redundant syntax

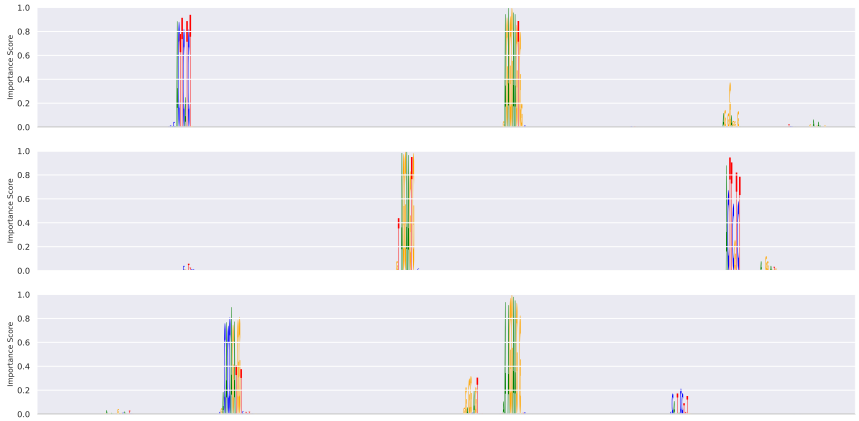

Figure 13: Inclusion scrambler importance scores for a repressive syntax

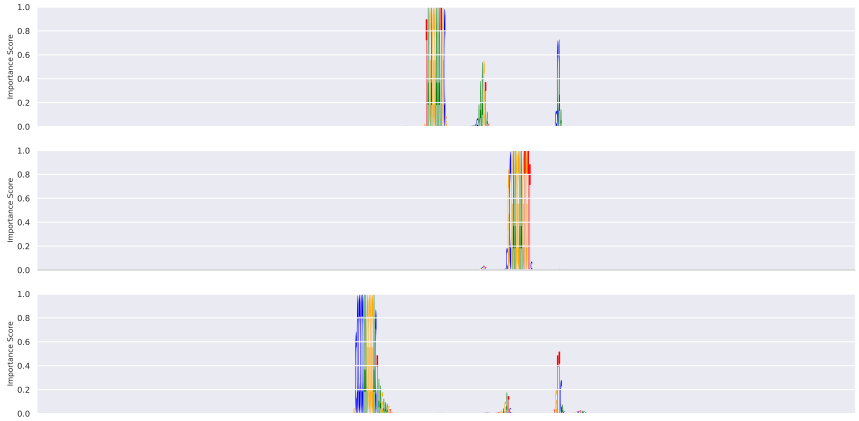

Figure 14: s-MEM importance scores for a repressive syntax

Figure 15: Occlusion scrambler importance scores for a repressive syntax

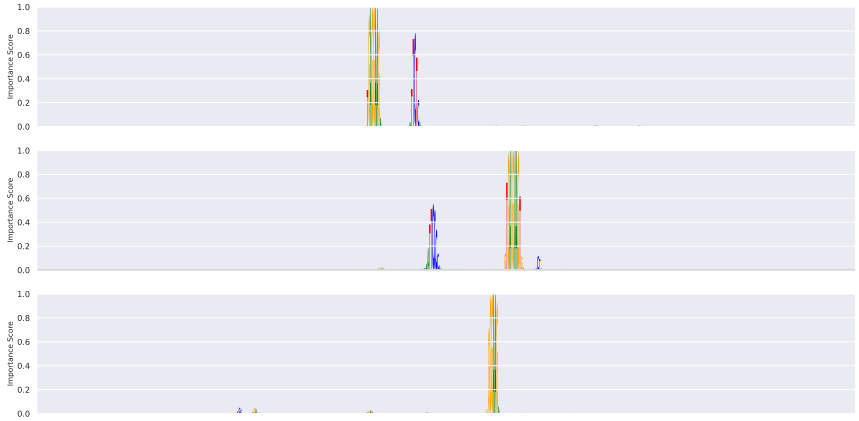

Figure 16: n-MEM importance scores for a redundant syntax